AFRL-AFOSR-JP-TR-2023-0078

Investigation on the Tuneable Optical Properties of Reformatted Bacterial Cellulose

Lim, Sierin
NANYANG TECHNOLOGICAL UNIVERSITY
50 NANYANG AVENUE
SINGAPORE, , 639798
SGP

04/17/2023
Final Technical Report

Air Force Research Laboratory
Air Force Office of Scientific Research
Asian Office of Aerospace Research and Development
Unit 45002, APO AP 96338-5002

REPORT DOCUMENTATION PAGE

PLEASE DO NOT RETURN YOUR FORM TO THE ABOVE ORGANIZATION.

1. REPORT DATE	2. REPORT TYPE	3. DATES COVERED	
20230417	Final	START DATE 20190829	END DATE 20220828

4. TITLE AND SUBTITLE
Investigation on the Tuneable Optical Properties of Reformatted Bacterial Cellulose

5a. CONTRACT NUMBER	5b. GRANT NUMBER	5c. PROGRAM ELEMENT NUMBER
	FA2386-19-1-4060	
5d. PROJECT NUMBER	**5e. TASK NUMBER**	**5f. WORK UNIT NUMBER**

6. AUTHOR(S)
Sierin Lim

7. PERFORMING ORGANIZATION NAME(S) AND ADDRESS(ES)
NANYANG TECHNOLOGICAL UNIVERSITY
50 NANYANG AVENUE
SINGAPORE 639798
SGP

8. PERFORMING ORGANIZATION REPORT NUMBER

9. SPONSORING/MONITORING AGENCY NAME(S) AND ADDRESS(ES)	10. SPONSOR/MONITOR'S ACRONYM(S)	11. SPONSOR/MONITOR'S REPORT NUMBER(S)
AOARD UNIT 45002 APO AP 96338-5002	AFRL/AFOSR IOA	AFRL-AFOSR-JP-TR-2023-0078

12. DISTRIBUTION/AVAILABILITY STATEMENT
A Distribution Unlimited: PB Public Release

13. SUPPLEMENTARY NOTES

14. ABSTRACT
The investigations suggest the type of drying process and incubation period can alter the optical and material properties of bacterial cellulose.• Press dried films showed better optical transmission as compared to freeze dried films but lower reflectance. • Material characteristics of press dried films differed from freeze dried films, nanofibers were compactly packed and displayed lower crystallinity.
• The DOE investigations suggest that only certain factors affect BC microparticles yield and uniformity, while other factors set to a constant value. • Media flow rate, incubation type and bacteria ratio affect BC microparticle yield significantly. • Optimum harvest of inclusion bodies is crucial to ensure high yield of reflectin protein.• Purification of reflectin protein through FPLC is not as effective as the HPLC method as performed in previous literature. • BC biofunctionalization using co-culture of E. coli secreting m6A-curli peptides was
successful.
Key Achievements reported:•
Obtained optimum film thickness for optical tunability; optical transmission was better when the films were press dried.
• Identified parameters for producing increased amount of bacterial cellulose microspheres with good size control through detailed Design of Experiment studies.
• Purified reflectin protein

15. SUBJECT TERMS

16. SECURITY CLASSIFICATION OF:			17. LIMITATION OF ABSTRACT	18. NUMBER OF PAGES
a. REPORT	b. ABSTRACT	c. THIS PAGE		
U	U	U	SAR	18

19a. NAME OF RESPONSIBLE PERSON	19b. PHONE NUMBER *(Include area code)*
JEREMY KNOPP	315-227-7006

Standard Form 298 (Rev.5/2020)
Prescribed by ANSI Std. Z39.18

Final Report

Air Force Office of Scientific Research
IOA Asian Office of Aerospace Research and Development
(PKG00249988)

Investigation on the Tunable Optical Properties of Reformatted Bacterial Cellulose (WS00321463)

Principal Investigator: Sierin Lim
Research Staff: Vishnu Vadanan Sundaravadanam

School of Chemistry, Chemical Engineering and Biotechnology
Nanyang Technological University
Singapore

Table of Contents

This document contains 5 sections.

SECTION I: DETAILS OF PROJECT

a) Award No.	FA2386-19-1-4060
b) Project Title	Investigation on the Tuneable Optical Properties of Reformatted Bacterial Cellulose
c) Salutation of Lead PI	Associate Professor
d) Name of Lead PI	Sierin Lim
e) Host Institution	Nanyang Technological University
f) Department	School of Chemical and Biomedical Engineering
g) Approved Budget (inclusive of Indirect costs – if any)	$150,000.00 ($75,000.00 + $75,000.00)
h) Duration of Project	2019-2023
i) Project Start Date	29-Aug-2019
j) Project End Date	31-Aug-2022

SECTION II: BUDGET AND EXPENDITURE

Start Date	End Date	Direct Cost ($)	Indirect Cost ($)	Total Cost ($)
29/08/2019	28/02/2022	170,443.75	34,088.75	204,532.50

Category	WBS Number 04OGP000022C110	Budget (S$)	Expenditure (S$)
Expenditure on Manpower	EOM01	145,575.93	144,993.98
Equipment	EQT01	4,815.00	4,815.00
Materials and consumables	MAC01	11,871.54	11,848.35
Other Operating Expenses	OOE01	8,181.28	8,181.28
Overseas Travel	0OST01	0.00	0.00
Indirect Cost	IRC01	34,088.75	17,118.75

SECTION III: PROJECT UPDATE

Investigation on the optical properties of bacterial cellulose-based materials

Abstract

Among the many tunable properties of bacterial cellulose (BC), their optical properties – especially those that pertain to the molecular level organization – remain sparsely investigated. The bulk of the past studies have focused on a single approach to manipulate optical properties: the use of external force to align BC fibres as they are excreted from the bacteria. Recently, we have developed two new approaches that enable systematic control of the optical properties of BC. These include (1) reformatting BC fibres using a microfluidic device and (2) the chemical treatment for fibrillation process. In the microfluidic approach, we have shown that by templating the bacterial growth within the pore confinements of the porous agarose microspheres, controlled reformatting and rearrangements of the BC nanofibers can be achieved. Subsequent removal of the sacrificial agarose template gives rise to microspheres of BC, which display a strikingly translucent optical characteristic. In our chemical treatment approach, we have shown that the use of TEMPO, an oxidizing agent, in conjunction with ultrasonication, allows to produce soluble BC with distinct optical properties. Although the two approaches are successful in tailoring the optical properties of BCs, the underlying molecular mechanisms are not known, deciphering which is the main goal of this proposal. We **hypothesize** that the modified optical properties emerge in the micro-confinement and chemical treatments emerge by a common mechanism. In both cases, the molecular level self-assembly changes the sizes, distributions, and arrangements of BC fibres, which in turn alters the refractive index characteristics of BCs. To test this hypothesis, we **propose** to systematically modify and reassemble BC fibres to examine in detail how fibre arrangements, crystallinity, and sizes influence the refractive index and generate an elemental map correlating structural attributes with optical properties.

Key achievements

- Obtained optimum film thickness for optical tunability; optical transmission was better when the films were press dried.
- Identified parameters for producing increased amount of bacterial cellulose microspheres with good size control through detailed Design of Experiment studies.
- Purified reflectin protein from squid for future incorporation into bacterial cellulose microspheres.

Specific aims

The specific aims of the proposed project were:

1. Investigate the effects of hydration layers on the fibers by
    a. Applying different drying methods that are freeze drying and press drying.
    b. Modifying film thickness
2. Increase yield and size uniformity of bacterial cellulose microspheres:
    a. Conduct Design of Experiments (DOE) study to optimize the factors responsible for BC microspheres production.
    b. Characterize the produced microspheres.
3. Produce and incorporate reflectin protein in BC microspheres
    a. Increase the yield of squid reflectin protein for tunable optical properties.
    b. Incorporate the reflectin protein in BC microspheres for optical applications.
4. Bioengineer hybrid functional bacterial cellulose films
    a. Fuse m6A peptide to curli secretory protein to template magnetite nanoparticle synthesis.
    b. Coculture *E. coli* secreting m6A-curli with BC to obtain magnetic BC

Approaches

There are two approaches to the project: (1) BC microsphere production and reflection protein production scale-up and (2) Biofunctionalization of BC using m6A-curli.

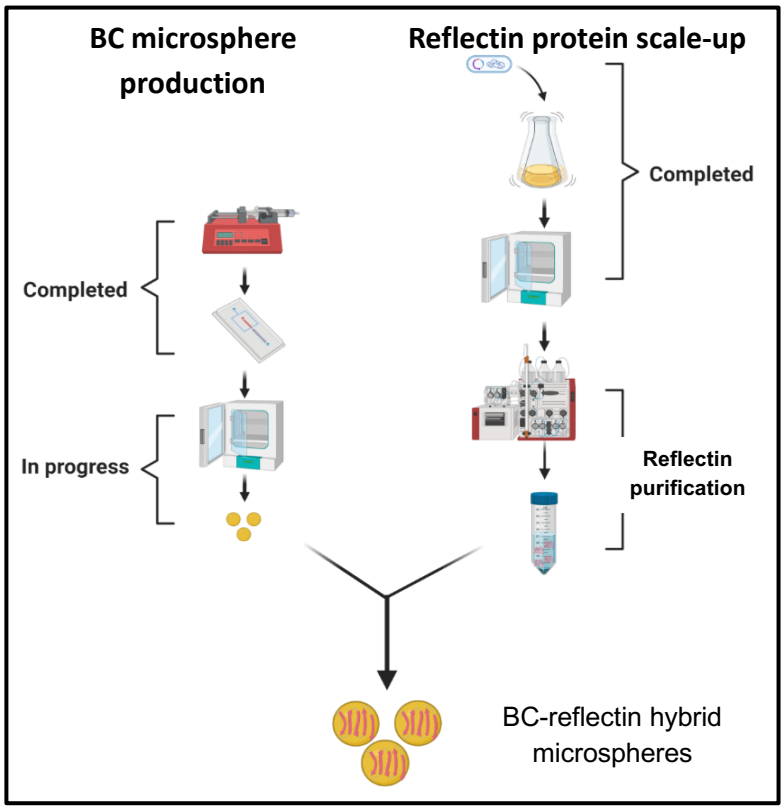

Figure 1: Schematic representation of the production and incorporation of bacterial cellulose microspheres and squid reflectin protein to form hybrid microspheres with tunable optical properties.

General Methodology

Film production and functionalization

1. Incubate bacteria in carbon source rich media for different period and harvest films of varying thickness.
2. Use different drying processes to investigate the material and optical properties of the films (hydraulic press dry and freeze dry).
3. Biofunctionalize BC using m6A-curli peptides.

Microsphere production and reflectin incorporation

1. Design a Plackett-Burman study to screen the various production variables.
2. Minimize the reflectin protein loss by optimizing the purification/harvest protocols.
3. Drop cast the reflectin protein on BC microspheres thin films.

Optical properties determination

4. Determine transmission of the film format.

Design of Experiment (DOE) methodology for production optimization

This project aims to optimise the production of bacterial cellulose solid microspheres by maximising yield and ensuring uniformity. Thus, five variables were chosen to investigate the response pattern and to determine the important factors that affect the two output response variables (yield and uniformity).

In this study, the 12-run Plackett-Burman screening design is used to investigate the main factors that have a significant impact on the output variables – yield and uniformity. The factors and their high and low levels, coded as -1 and +1, were media flow rate (A; 4, 10), oil flow rate (B; 15, 20), incubation period (C; 5, 10), incubator type (D; static, agitated) and bacteria ratio (E; 1:19, 1:9) are shown in Table 1. Each experimental condition was repeated twice.

The resultant BC microspheres produced under the conditions stated by the DOE design matrix are then harvested and stained with Calcofluor White Stain for quantitative analysis via flow cytometry.

Table 1. Factors and the two levels used in DOE Symbol

Factors	Low (-1)		High (+1)
Media flow rate	A	4	10
Oil flow rate	B	15	20
Incubation period	C	5	10
Incubator type	D	Static	Agitated
Bacteria ratio	E	1:19	1:9

Results and Discussions

To establish the baseline for the project, we performed basic investigations on the optical properties of BC films. These results would serve as a reference for future development of hybrid BC based materials in this work.

Press dried films and surface morphology

BC films were dried using two techniques, press-drying, and freeze-drying. Various dried films are shown in Figure 1. Films grown for 5 days were thinner than those grown for 10 days. In hydrated state, the 5-day films appear to be more transparent compared to the 10-day films. The observation was expected as the thinner film would scatter less of the incident light compared to the thicker films. Freeze-drying method produced sponge-like opaque BC films and will not be considered for future investigations. Two drying temperatures were explored for press drying (i.e. 50°C and 100°C). The hydrated BC films were press dried at 50 °C and 100 °C for one hour. Temperature controlled hydraulic press drying method produced translucent BC films. The observation was consistent when scaled-up from 12-well plate culture plate to 35-mm petri dish.

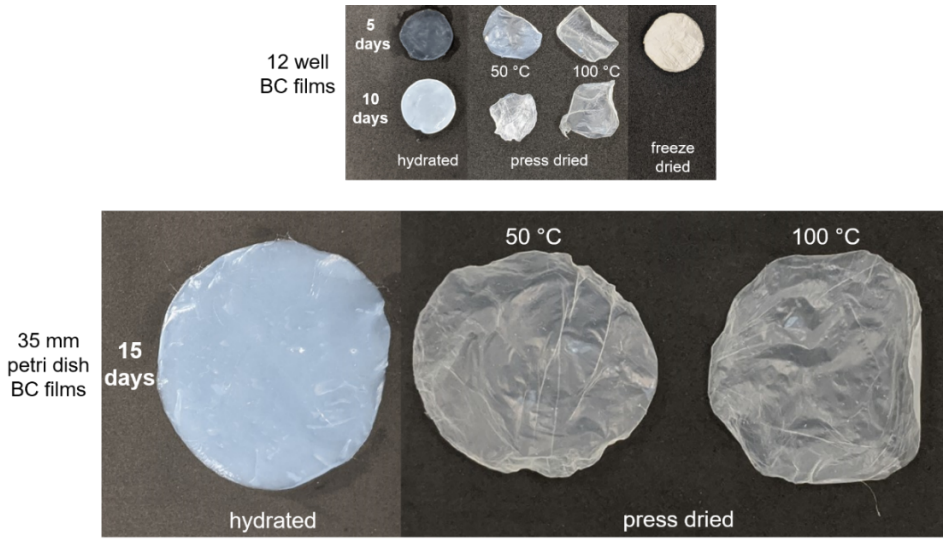

Figure 1: BC films grown in different containers (top: 12-well culture plate and bottom: 25-mm petri dishes). The 12-well samples were grown for 5 and 10 days. The longer growth time resulted in thicker films. The samples were dried using two different techniques that were press-drying and freeze-drying. The press-drying were performed at two different temperatures (50 °C and 100 °C). The images are presented to scale.

Surface morphology of BC films under various drying methods

Surface morphology of the press dried films remain same irrespective of the incubation period and temperature (Figure 2). Structural morphology of press dried films varies with freeze dried films with distribution of pores across the matrix. Press dried films display compact packing of the 30nm cellulose nanofibers across the matrix with minimal pore distribution. Surface morphology of the freeze-dried films displayed the characteristic porous network due to the presence of water molecules in the films prior to drying. When the water molecules were removed through freeze drying it contributed to formation of pores in the dried films. The compact packing of the nanofibers in the press dried films contributed to the transparency of the final dried film as seen in figure 1.

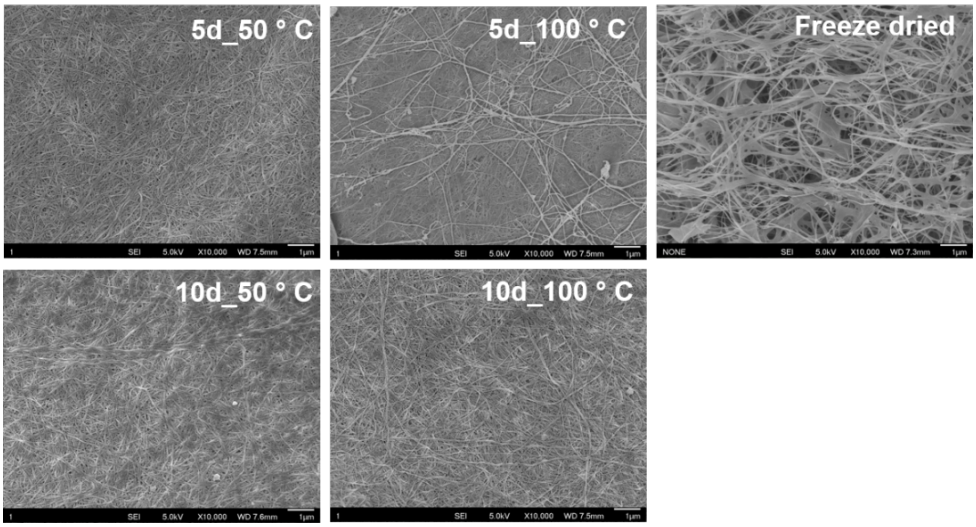

Figure 2: Electron micrographs of the 5-day and 10-day films press-dried at 50°C or 100°C. Freeze-drying was performed on 5-day film. All films were grown in 12-well plate culture plates. Scale bars are 1 μm.

Crystallinity and chemical compositions of BC films

The crystallinity and chemical compositions of BC films were determined using X-ray diffraction and IR spectroscopy, respectively. Analysing the XRD patterns, broad diffraction peaks at 15° and 22.5° suggested that the BC films were of cellulose type I. These peaks are assigned to the characteristic interplane distances of cellulose 1α and 1β phases. Cellulose type I patterns were observed for all the dried films, confirming that BC structure is preserved during the drying process. Meanwhile, a difference can be observed in the relative intensity of the BC peaks, suggesting a change in the orientation of the cellulose nanofibers during press drying, thereby displaying lower crystallinity as compared to the freeze dried film. Lower incubation period also contributed to decreased crystallinity in the final dried films due to the limited time available for the formation of inter and intramolecular hydrogen bonds.

IR spectroscopy indicates that the transparent press-dried films scanned through ATR mode, display very low reflection as most of the signal is transmitted through the films whereas, the freeze dried film displayed all the signature peaks of BC. This indicates that IR spectroscopy may not be a suitable method to characterise the chemical structure of the final press dried films in the future.

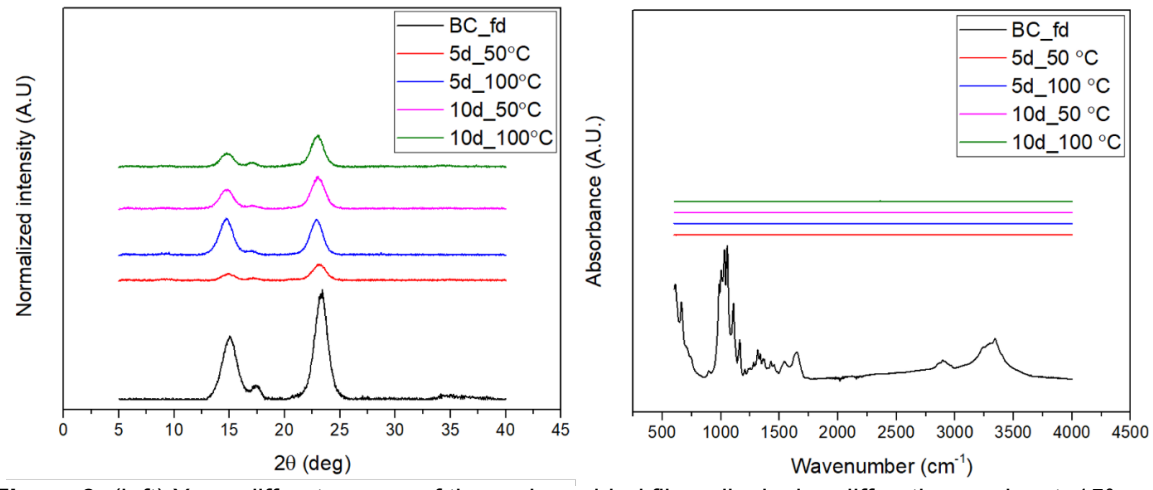

Figure 3: (left) X-ray diffractograms of the various dried films displaying diffraction peaks at 15° and 22.5°. (right) IR spectroscopy of the various dried films with press dried films showing no absorbance.

Optical characteristics of dried BC films

Optical properties of the dried films were analysed using a spectrophotometer. Press-dried transparent films showed better transmittance than opaque freeze-dried film in the visible region with 50-80% transmittance. Films with 5 days incubation period showed better transmittance than 10 days films, due to lower fibre production and packing across the matrix. The high transmittance is primarily due to the lateral size of the nanofibers present in the press dried films and the light scattering is also avoided by the nanofibers, which are smaller than the wavelength of light. All the press dried transparent films as expected showed low reflectance of about 1-5% in the visible and infrared region since most of the light is transmitted through the films.

Opaque freeze-dried film offered a better reflecting surface than the transparent press dried films but showed very low or no transmittance in the visible and infrared region. The transparency shown by pristine press dried films in the visible and infrared region of the electromagnetic spectrum make them suitable substrates for optical applications as flexible displays, optical fibres and sensors.

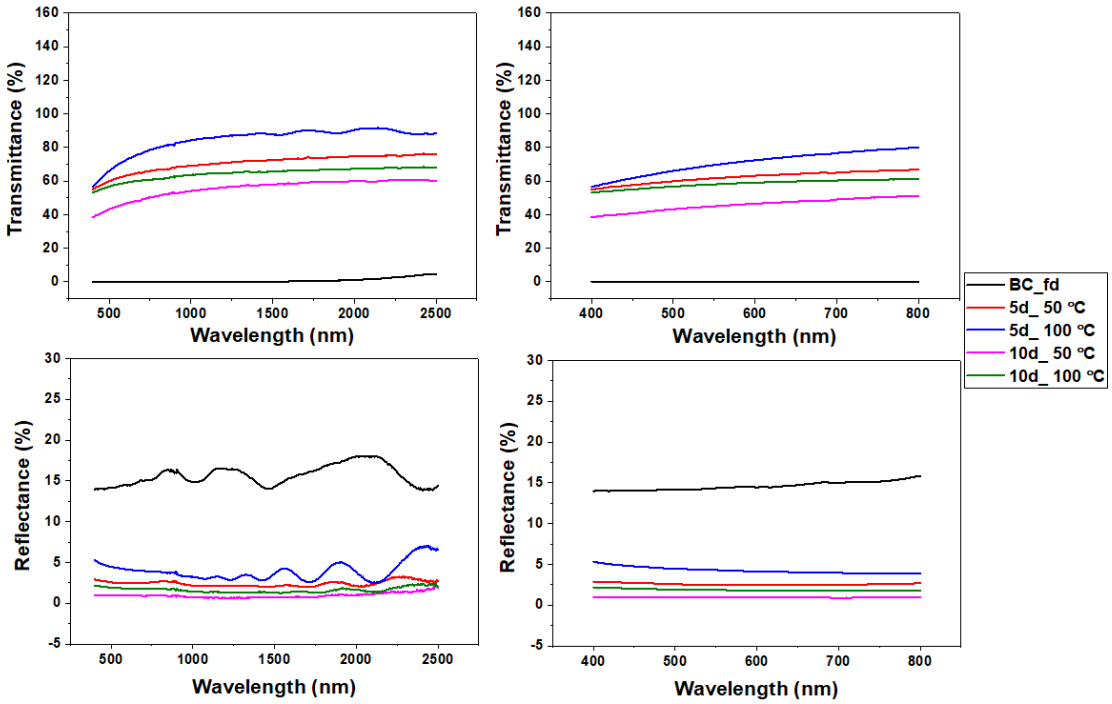

Figure 4: (top) Transmittance signals of the dried films in visible and IR spectrum. (bottom) Reflectance signals obtained from the various dried films using spectrophotometer.

Bacterial cellulose microspheres

This section will discuss the results obtained for bacterial cellulose microspheres and optimisation of the production conditions for improved yield and uniformity.

Characterisation of agarose cores and BC microspheres

The agarose core with bacteria are typically be sandwiched between the oil and water phases as shown in Figure 2. To ensure that bacteria is encapsulated in all the microspheres produced, confocal imaging is performed to measure the RFP-fluorescence from the RFP-tagged bacteria strain. As shown in Figure 3, each microsphere is shown to have red fluorescence, which suggests that bacterial encapsulation is successful.

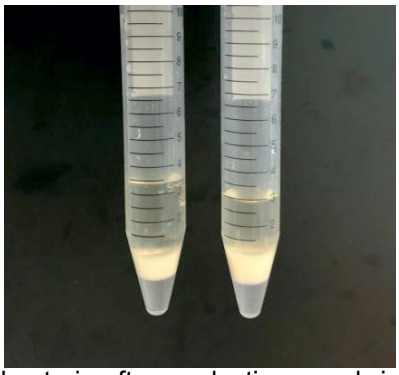

Figure 2: Agarose cores with bacteria after production, sandwiched between the water and oil phases

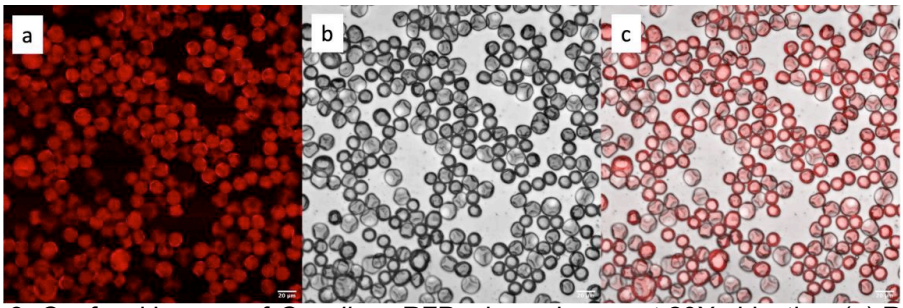

Figure 3: Confocal images of *G. xylinus*-RFP microspheres, at 20X objective. (a) RFP, (b) Brightfield, (c) Compositive of RFP and brightfield

The BC microspheres were heat-treated with 1% NaOH, removing the bacteria cells thus eliminating the RFP from the sample. The resultant sample were then stained with Calcofluor White Stain (Sigma Aldrich) and 10% KOH for the detection of cellulose. The stained BC microspheres were then imaged using confocal microscopy as shown in Figure 4. The samples were also characterised via Scanning Electron Microscope (SEM) to observe the network structure in the BC microspheres (Figure 5).

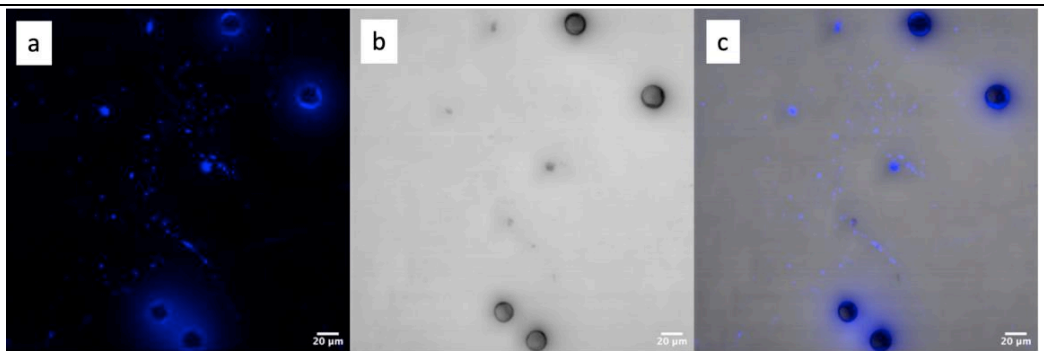

Figure 4: Confocal images of BC microspheres stained with Calcofluor White, at 20X objective. (a) DAPI, (b) Brightfield, (c) Composite of RFP and Brightfield

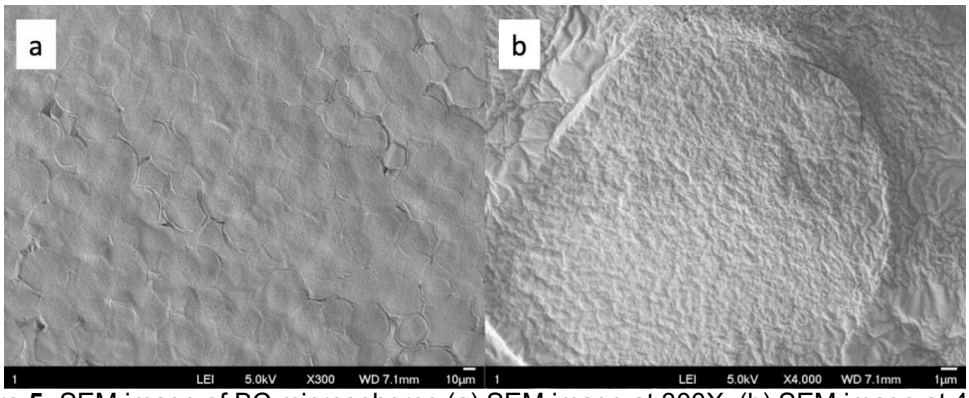

Figure 5: SEM image of BC microspheres (a) SEM image at 300X, (b) SEM image at 4000X

DOE analysis

The defined experimental design and the response levels obtained for each experimental run are recorded in Table 2 and was analysed using DOE software.

Table 3. Experimental run conditions and the output response

	Factors					Output	
Run	**A**	**B**	**C**	**D**	**E**	**Yield (x10^5)**	**Uniformity (%)**
1	−1	1	−1	−1	1	0.39	97.5
2	1	−1	1	−1	1	23.5	92.1
3	−1	−1	−1	1	−1	2.46	81.3
4	1	1	−1	1	−1	8.93	90.4
5	−1	−1	1	1	−1	3.70	87.1
6	−1	1	1	−1	−1	0.84	97.9
7	−1	−1	−1	−1	1	1.95	94.7
8	1	−1	1	1	1	23.8	56.4
9	1	−1	−1	−1	−1	6.72	83.6
10	1	1	−1	1	1	14.0	81.1
11	−1	1	1	1	1	4.00	98.0
12	1	1	1	−1	−1	16.1	97.6

The resultant values of yield and percentage uniformity are input into the DOE design matrix to generate the standardised effects and screener plot graph via the Minitab software. These effects are reflected through the Pareto chart and the main effects screener plot for both yield and uniformity.

With reference to the Pareto chart in Figure 6a, it is inferred that factors A, C and E have significant impacts on yield, each of them having factor effect value greater than 2.45. Factor A has the most effect on yield, followed by C and E. The main effects screener plot in Figure 6b shows a positive effect across all factors, apart from factor B. It is noted that factor B has a negative effect on yield.

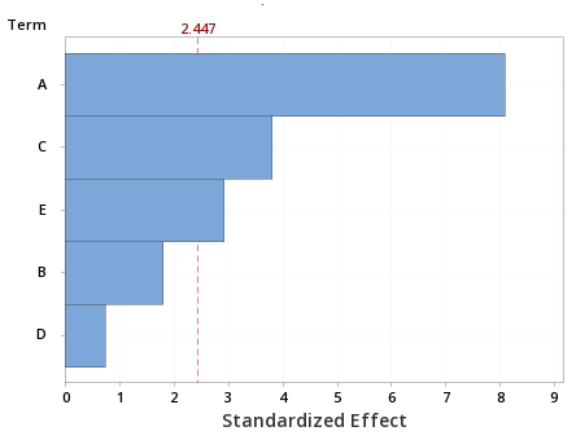

Figure 6a. Pareto chart for the standardised effect for yield

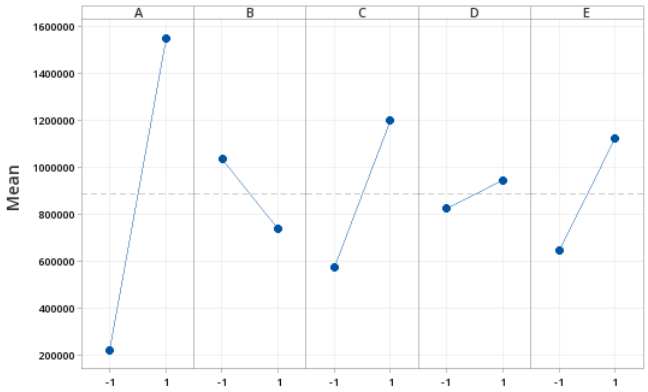

Figure 6b. Main effects screener plot for yield

In terms of uniformity, the Pareto chart (Figure 7a) shows that none of the factors played a significant part in ensuring uniformity, with all the factor effect values falling below 2.45 and factor C having no effect on uniformity. The main effects screener plot (Figure 7b) shows a steep-line relationship for factor A, B and D but their main screener effect of these factor remains zero, since the overall mean uniformity remains high.

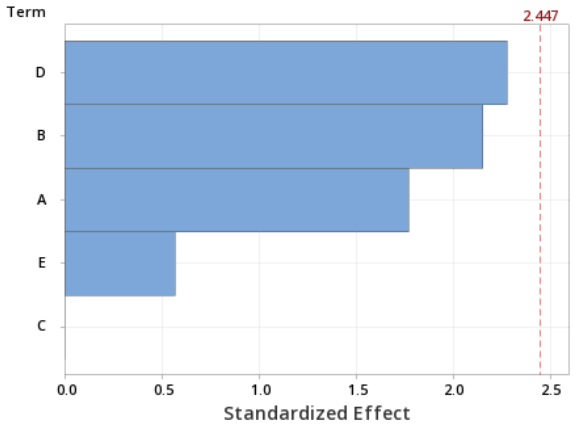

Figure 7a. Pareto chart for the standardised effect for uniformity

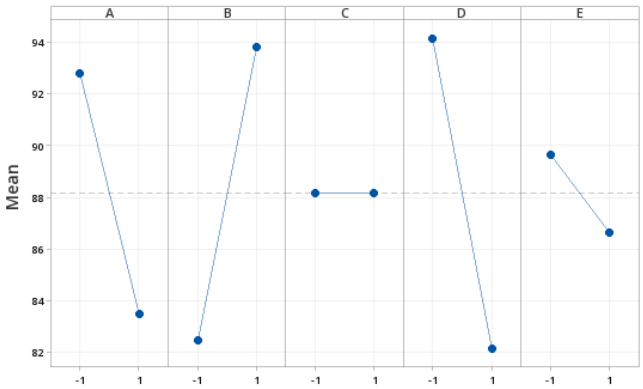

Figure 7b. Main effects screener plot for uniformity

Upon analysis of the main effects from the design of experiment, it is concluded that factors A, C and E; namely the media flow rate, incubation period and the media to bacteria ratio has the more significant impacts on the output variables. Since the oil flow rate (factor B) has a negative effect on yield and incubator type (factor D) has little or no effect on the response levels, these factors can be removed from the DOE design matrix for the further investigation of the significant effects.

Reflectin protein production

This section will discuss the production and purification of the reflectin protein

Production and purification of reflectin protein

Reflectin A1 gene from squid *Doryteuthis pealeii* was cloned into a pET28a expression vector containing N-terminal histidine tag via restriction enzyme digestion.

The protein solution were applied to the HisTrap High Performance column using ÄKTA go (Cytiva) fast protein liquid chromatography (FPLC) system (Figure 8). Standard protocols for the affinity chromatography were used. The purity, molecular weight of reflectin, post washing and affinity chromatography were visualized using SDS-PAGE. As expected, a 40 kDa band could be observed in Figure 9 in lane 2 which indicates that reflectin has been successfully purified.

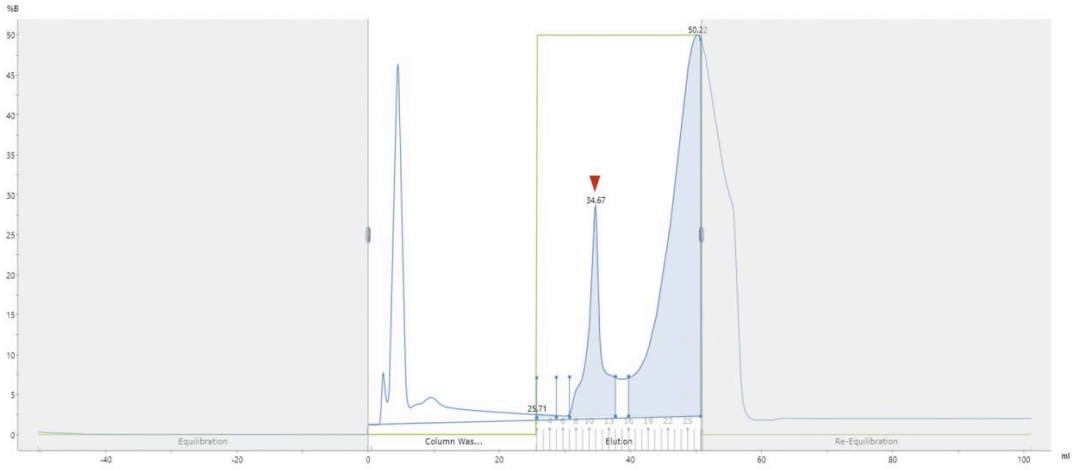

Figure 8: Chromatogram result of HisTrap High Performance column chromatography purification of reflectin A1. Fraction 10, the peak of the elution step indicated by the red arrow, was collected, and analysed by SDS-PAGE.

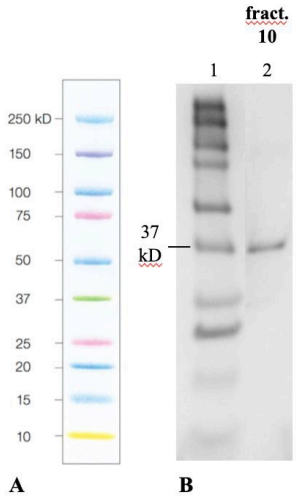

Figure 9: The analysis of purification of reflectin A1 via SDS-PAGE (A) Representative plot of Precision Plus Protein Kaleidoscope standard (B) The individual lanes are: lane 1, 10 – 250 kDa molecular weight standards; lane 2, purified reflectin from FPLC eluted fraction 10 from FPLC

Characterisation of reflectin protein

Reflectin protein was characterised based on their concentration, size distribution and secondary structure.

Bradford assay was performed to determine the concentration of the purified reflectin protein. Purified reflectin protein has an average concentration of **0.247 mg/mL.** Dynamic light scattering (DLS) analyses are commonly used to detect aggregates in macromolecular solutions and determine the size of proteins. In this work, DLS was used to observe any difference in size distribution between reflectin samples at different pH. With reference to Figure 10, reflectin protein has a smaller size of approximately 8 nm for pH 5 and 10 nm for pH 7. Meanwhile, at higher pH, the reflectin protein samples have a larger size of approximately 800 nm for pH 11 and 1000 nm for pH 9. It can be concluded that as the pH increases, the reflectin proteins tend to aggregate, resulting in the larger size distribution.

Circular dichroism was applied to determine the secondary structure of proteins. Different structural elements have characteristic circular dichroism spectra, as seen in Figure 12. With reference to Figure 11, no conclusive secondary structures could be inferred for reflectin samples pH 5, 9 and 11. However, for pH 7, a slight alpha helical structure can be concluded as it has similar shape as the alpha helical structure of the standard CD spectrum which is characterized with negative bands at approximately 222 nm and 208 nm. Since reflectin protein sample with pH 7 is the sample with the most defined secondary structure, this pH was used for the incorporation of reflectin into bacterial cellulose microspheres.

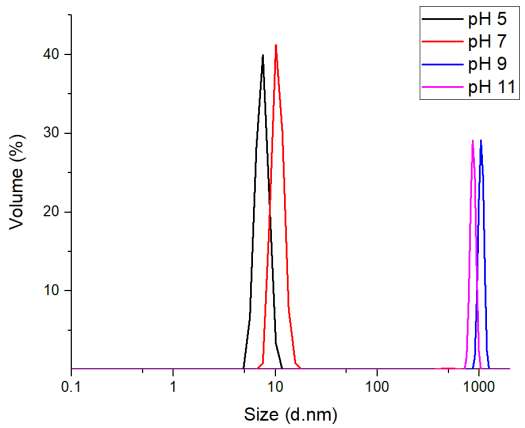

Figure 10: Dynamic light scattering of reflectin A1 protein samples at pH 5, 7, 9 and 11

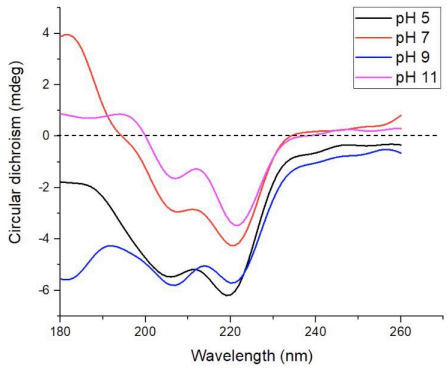

Figure 11: A representative circular dichroism spectrum obtained for reflectin A1 (approximately 0.2 mg/mL) at pH 5, pH 7, pH 9 and pH 11

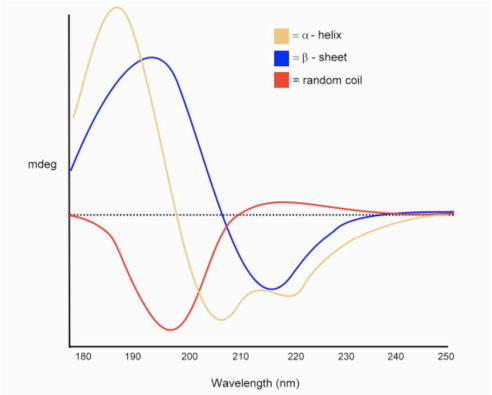

Figure 12: A standard circular dichroism spectrum for secondary structures of protein, such as alpha-helix, beta-sheet and random coil

Incorporation of reflectin and bacterial cellulose microspheres

Pure bacterial cellulose microspheres solution was casted and dried on a hydrophobic surface and a thin film of microspheres was then recovered as seen in Figure 13. Based on this result, the same method was done to the bacterial cellulose and reflectin protein mixture as recovery of a thin film is required for refractive index measurement. Refractive index measurement is essential in determining how the incorporation of reflectin protein has modified the optical properties of bacterial cellulose microspheres. However, after incorporation of reflectin into bacterial cellulose microspheres, it was found that the solution was too thin and had spread out on the hydrophobic surface. The resulting film was thin and attempts to peel the film resulted in a powder like material, as seen in Figure 14. This could be due to the low concentration and short incubation period of bacterial cellulose microspheres used in the incorporation study. Thus, refractive index measurement could not be performed.

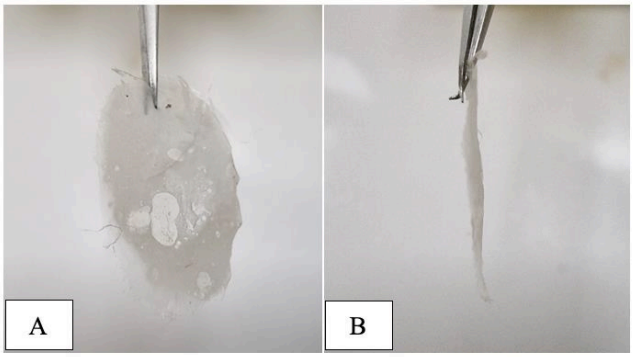

Figure 13: Pure bacterial cellulose microspheres film after drying on hydrophobic surface (A) front view (B) side view

Figure 14: Incorporation of reflectin protein onto BC microspheres and casted on hydrophobic surface

Bioengineered hybrid functional bacterial cellulose

As a proof of concept, we demonstrated that entrapped recombinant *Escherichia coli* in cellulose matrix produced by *Gluconacetobacter* aided in functional display with tunable capacity. The recombinant *E. coli* contained the genetic circuit, amyloid curli proteins, CsgA tagged with short functional m6A peptide domains, were responsible for *in situ* magnetite nanoparticle nucleation. The functional amyloid CsgA proteins were secreted extracellularly by *E.coli* and self-assembled in the cellulose matrix. The injection of functional amyloid proteins into cellulose facilitated magnetite nanoparticle decoration across the matrix. Through this bioengineered design we were able to achieve a maximum magnetization of 40 emu g^{-1}.

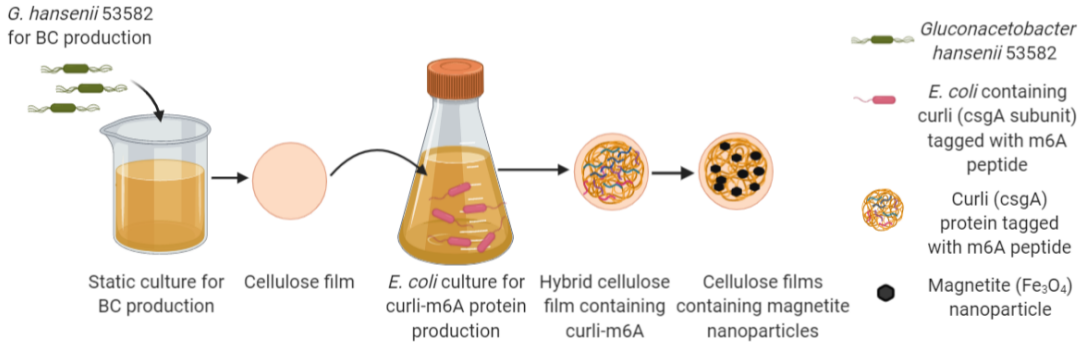

Schematic illustration of the preparation of functional hybrid cellulose films. *Gluconacetobacter hansenii* 53582 was used to produce cellulose films. The cellulose films were transferred to recombinant *E. coli* cultures producing curli subunit (csgA) with magnetite nucleating peptides to functionalise the cellulose films. Particles with uniform size and shape were produced in the presence of the hybrid cellulose-curli(m6A) films.

The BC membranes did demonstrate limitations in nanoparticle templating (Figure 15) due to the limited distribution of pores and the availability of hydroxyl groups for nucleation and growth. The bottom side is limited to the process of nanoparticle synthesis as they are not in direct contact with the iron salt that is injected. The bulk material is not black but the nanostructural morphology of the material under SEM confirmed the presence of magnetite nanoparticles on either side of the cellulose films (Figure 16). Further optimization of the mixing and reaction conditions would eliminate these issues and lead to a more uniform material formation.

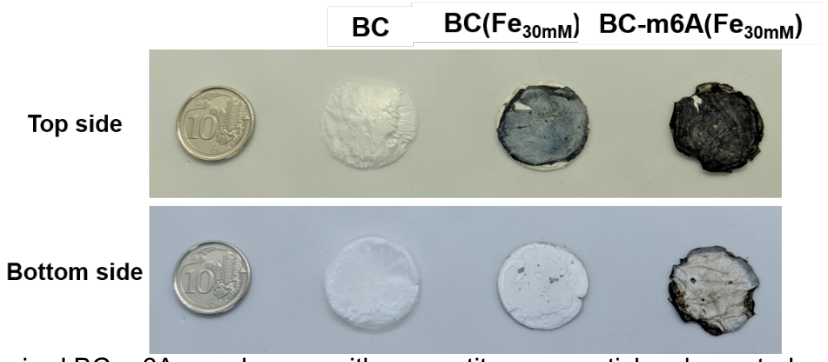

Figure 15. Bioinspired BC-m6A membranes with magnetite nanoparticles decorated across the membrane.

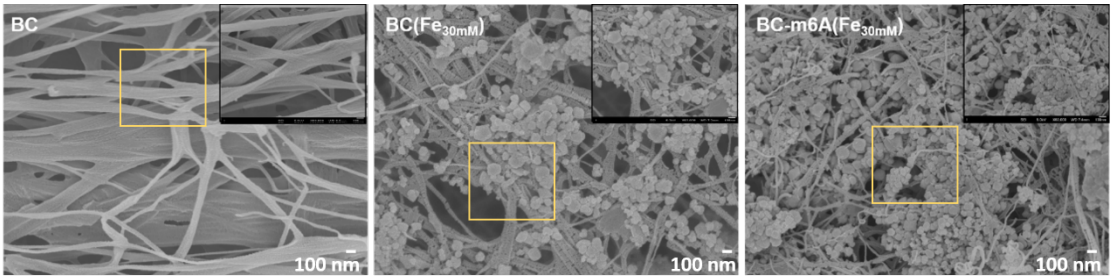

Figure 16. Structural morphology of various cellulose membranes. (a) BC, (b) magnetic BC and (c) magnetic BC-m6A (*Scale bar: 100 nm*).

Magnetic M *versus* H curves at room temperature was measured for all the membranes (Figure 17). As expected, the pristine BC film did not demonstrate any magnetic behaviour. With the incorporation of magnetite nanoparticles both the magnetic membranes displayed superparamagnetic behaviour. Superparamagnetic behaviour is characterized by the lack of hysteresis loop and low/no coercivity. The saturation magnetization (M_s) of BC-m6A was four times greater than BC films deposited with nanoparticles. The high M_s of 40 $emug^{-1}$ was due to the higher concentration of magnetite nanoparticles homogeneously dispersed across the matrix, as observed in FESEM.

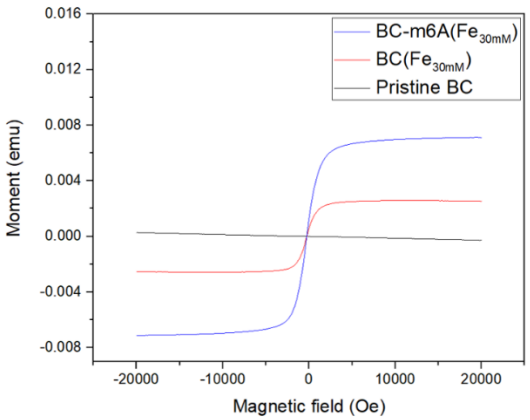

Figure 17. VSM measurements of magnetic BC and magnetic BC-m6A membranes

The biological approach employed in this study is synonymous to a bottom-up approach wherein, the bacteria are responsible for providing the base matrix as well as incorporating functionality to the matrix. The bioengineered functional cellulose membranes are comprised of bacterial cellulose and amyloid fusion protein CsgA genetically tagged with m6A peptide domain. The resulting BC scaffold network maintained its ability to trap recombinant *E. coli* bacteria within its matrix. This supports the uniform intercalation of the amyloid protein with BC nanofibers, as not observed in previous cellulose composite design approaches. The m6A peptide domains added functionality to the cellulose matrix without any harsh chemical or mechanical processes.

Problems/Challenges

- Realignment of cellulose nanofibers for tunable optical properties through mechanical and chemical treatment: The disintegration of nanofibers through these modification processes caused the disruption of the inherent structural properties of BC. The treatments resulted in compromised mechanical properties and crystallinity of the BC films which were undesirable for applications. Hence the films were freeze dried and press dried to check the influence of packing density for optical tunability.

- The water insoluble nature of BC films made it challenging to produce and design hybrid materials: BC microspheres produced in this work have been shown to potentially overcome this problem by forming the fibrils through a bottom-up approach. It is also expected that this micro-confinement will further aid in the intercalation of polymers, nanoparticles to form hybrid functional microspheres.

- Inclusion body purification and harvest had lot of protein loss at various washing steps. Further optimisation of inclusion body wash can lead to better reflectin protein yield.

- Purification of reflectin protein through fast protein liquid chromatography was successful for small amounts but had issues during scale up. Further investigation on the purification strategies either HPLC or FPLC could be tested for reflectin purification.

Conclusion

- The investigations suggest the type of drying process and incubation period can alter the optical and material properties of bacterial cellulose.

- Press dried films showed better optical transmission as compared to freeze dried films but lower reflectance.

- Material characteristics of press dried films differed from freeze dried films, nanofibers were compactly packed and displayed lower crystallinity.

- The DOE investigations suggest that only certain factors affect BC microparticles yield and uniformity, while other factors set to a constant value.

- Media flow rate, incubation type and bacteria ratio affect BC microparticle yield significantly.

- Optimum harvest of inclusion bodies is crucial to ensure high yield of reflectin protein.

- Purification of reflectin protein through FPLC is not as effective as the HPLC method as performed in previous literature.

- BC biofunctionalization using co-culture of *E. coli* secreting m6A-curli peptides was successful.

SECTION IV: IMPACTS

Development of the principal discipline(s) of the project

This grant provided an opportunity to establish a reliable and robust platform for the synthesis of microparticles with good size control. The platform developed could further be tuned to synthesize materials with varied properties that could suit multiple applications in future investigations.

The co-culturing technique to produce hybrid BC through biofunctionalization was one of the firsts to show success with subsequent applications for wound healing under investigation.

Describe the impact in this reporting period on the development of human resources

The grant was an opportunity for a post doc to gain expertise in innovative strategies for microparticle synthesis and characterization. This was also an opportunity to train two final year project students and two, year 2 undergraduate students. One of the undergraduate students in currently continuing in the lab to work on the microsphere production while the other one is applying for a PhD.

SECTION V: DECLARATION AND ENDORSEMENT

a) Declaration by Lead PI

I declare that all of the above information provided is true and complete to the best of my knowledge.

Name Sierin Lim

Signature _____

Date 04-08-2022

b) Endorsement by Host Institution (Officer of Research/Executive Director of Research Institute)

Name _____

Designation _____

Signature _____

Date _____